Aust. J. Phys., 1977, **30**, 209–30

The Molonglo Deep Sky Survey of Radio Sources. I Declination Zone $-20°$

J. G. Robertson

School of Physics, University of Sydney, N.S.W. 2006.

Abstract

Results of a deep survey made at 408 MHz with the Molonglo cross are given. The catalogue lists positions and flux densities for a total of 373 radio sources, most of which have not previously been catalogued, in a solid angle of $0\cdot0201$ sr. This covers (with some excluded areas) right ascensions $01^{h}00^{m}$–$06^{h}44^{m}$ and $13^{h}45^{m}$–$17^{h}19^{m}$, with a range in declination of $41'$. Eighteen contour maps are given of sources that are extended or have very close companions. A thorough error analysis is given, as well as new operational definitions of completeness and reliability. The lower limit of flux density is 88 mJy, which is five times the r.m.s. error. An upper limit of 1000 mJy has also been imposed. Typical errors in positions are $15''$ at 100 mJy and $6''$ at 250 mJy.

1. Introduction

Four catalogues based on the general survey made with the Molonglo cross-type radio telescope have so far been completed (MCl: Davies *et al.* 1973; MC2 and MC3: Sutton *et al.* 1974; MC4: Clarke *et al.* 1976). These catalogues included sources with flux densities as low as $0\cdot2$–$0\cdot3$ Jy. The present deep survey is not a continuation of this series, but an attempt to reach significantly fainter sources in a small solid angle of sky, partly overlapping the MC1 region. A second instalment, at declination zone $-62°$, is presented in Part II (Robertson 1977*a*, present issue pp. 231–9). The number–flux density counts (and their corrections) are given in Part III (Robertson 1977*b* present issue pp. 241–9). The associated optical identifications are currently being carried out by H. S. Murdoch and G. L. White.

2. Observations

A short description of the Molonglo $1\cdot6$ km telescope and references to more detailed accounts have been given by Davies *et al.* (1973). Only a brief summary is given here. The telescope is a meridian transit instrument, providing a comb of 11 simultaneous pencil beams along the meridian, separated by half the beamwidth and spanning about $\frac{1}{4}°$ of declination in all. For the present survey, the beamwidth of an individual pencil beam was $2'\cdot66$ in right ascension and $2'\cdot97$ in declination, and the usual tapered aperture distribution was used. There are about 800 declinations to which the centre beam of the comb can be pointed (ranging from $\delta = +20°$ to the south celestial pole), each setting being known as a declination number. These are spaced to give a 50% overlap between adjacent declination numbers, with the result that all sources surveyed may be received on two adjacent settings. The output signal from each of the beams is integrated in 3 s intervals; the results are recorded on magnetic tape and are also displayed in analogue form on a facsimile recorder.

The sensitivity of the telescope varies in a periodic way with declination (Munro 1971). Both declination zones for the deep survey program were selected to lie at local maxima of the sensitivity. The deep surveys have the advantage of low noise preamplifiers on the north–south antenna and the availability of 3 combs of 11 beams, separated in right ascension by half the beamwidth. These facilities were not available at the time of the MC1, MC2 and MC3 surveys, and they provide a considerable improvement in sensitivity.

The observations were made in September 1973 over a period of 16 days, and consist of drift scans with the telescope set to one declination number during the transit of the right ascension range of the survey, and thus scanning a long narrow strip of sky. Seven adjacent declination numbers were observed in order to extend the declination coverage, each being observed twice to improve the sensitivity. The survey was made in two sections: 01^h–06^h and 13^h–17^h (the exact starting and ending right ascensions (1950·0) being $01^h\ 00^m\ 45^s$–$06^h\ 44^m\ 00^s$ and $13^h\ 45^m\ 40^s$–$17^h\ 19^m\ 15^s$). The gain of the telescope was monitored regularly by injecting a signal from a noise diode into the preamplifiers of the centre module of the telescope. This calibration procedure lasted about one minute, and obscured any source which transited during that period. For the survey observations, the calibration was inserted automatically once every sidereal hour. In addition, 16 calibration sources were observed every day to provide overall flux density and position calibration (see Section 4 below).

3. Analysis

(*a*) *Computer Reduction*

The recorded survey data contained multiple observations of each source owing to the 3 sets of 11 beams, the repeated observations of each declination number and the overlap of adjacent declination numbers. The data were averaged with respect to each of these redundancies, producing a set of 11 beam scans with the best possible signal to noise ratio for the available data. The computing was carried out on the KDF9 and Cyber 72 computers of the University of Sydney. In performing the above data averaging, there was a possibility of distortion of the final response if the individual responses occurred at significantly different positions. This could arise, for instance, as a result of position shifts due to electron density gradients in the ionosphere (Hunstead 1972). A check of the effects of such displacements showed that the resulting errors in flux density or position were negligible. Further details of this and other aspects of the data reduction have been given by Robertson (1976).

Source finding and fitting was performed using essentially the same computer program as for the MC1–MC4 catalogues. For each response that was stronger than a predetermined discrimination level, the program fitted a point source model and also calculated an integrated flux density. Because of the greater freedom allowed in calculating the integrated flux density, it has a much greater r.m.s. error than the flux density obtained from fitting the point source model, particularly when background confusion is significant, as in the present survey. For this reason, the latter was used for all but considerably extended sources (see subsection (*b*) below). This presents the possibility of introducing flux density errors due to partial resolution of sources, but the effect on the source counts is not significant (see Part III). The 'point source' flux density is not necessarily equal to the peak flux density—in fact it is the average of the peak and integrated flux densities (for slightly extended sources).

The discrimination level used in the source fitting was 80 mJy, but sources were only accepted for the catalogue above 88 mJy.

(*b*) *Manual Analysis*

For visual analysis and checking, the fully averaged data were optimally smoothed and plotted by computer as 11-beam line scans. Every response fitted by the source fitting program was inspected and, where necessary, flux densities were recalculated from the line scans. The scans were also inspected for sources missed by the source fitting program but which should be included in the catalogue. Seventeen such sources were found ($4\frac{1}{2}\%$ of the total number) and all were close to the lower limit of flux density.

In preparing the catalogue, the following criteria were used to make consistent decisions in ambiguous cases (consistency is particularly important because of the use of a Monte Carlo error analysis described in Section 6 below):

(i) In deciding whether two nearby peaks were adequately separated to be catalogued independently, a method based on a generalized Rayleigh criterion was used: if the flux density ratio of the peaks was between one and two, sources separated by less than $3'\cdot 8$ were considered unresolved, and were integrated together as one source. If the flux density ratio was between two and five, the critical separation was $4'\cdot 4$, while the very few cases of ratios larger than five were treated individually. Blending of nearby sources was not, however, a major problem (only 13 sources in the catalogue showing two peaks were integrated together on the above criterion). Integrated flux densities for these blends, and for other significantly broadened sources, were obtained by planimetry on the line scans.

(ii) A source was classed as significantly extended, and given an integrated flux density, only if the latter exceeded the 'point source' flux density by at least 50 mJy, which is $2\cdot 5$ times the r.m.s. error for the difference between integrated and point flux densities.

(iii) To avoid the possibility of including in the catalogue spurious responses of apparently significant integrated flux density but low 'point source' flux density, no source was included unless its 'point source' flux density exceeded the lower limit (88 mJy at $-20°$).

(iv) Sometimes, sources were not fitted well by the program; for instance, this could occur for sources close together but not blended. In such cases, a 'point source' flux density obtained from fitting by hand to the line scans was used in preference to the computed value, but only if the difference was greater than 15% for sources of less than 200 mJy, or 10% for those of over 200 mJy. The latter restriction was used to prevent the normal noise in flux density estimates from allowing unnecessary replacements of computed values. This same restriction was applied to the sources apparently missed by the program, since this could also be due to noise fluctuations. The positions fitted by the program were assessed similarly, and replaced by positions from the line scans or contour plots (described in Section 5 below) only if the coordinates differed by more than 10″. Notes are given in the catalogue when any quantity has been replaced in this way.

The precise declination limits of the survey were applied at this stage, the edges being $\delta(1973\cdot8) = -19°\,51'\,38''$ and $-20°\,33'\,07''$.

Table 1. Right ascensions (1950·0) excluded from catalogue

R.A. range		R.A. range		R.A. range		R.A. range	
h m s	h m s	h m s	h m s	h m s	h m s	h m s	h m s
			01ʰ–06ʰ Section				
01 05 17 to	01 06 17	02 14 42 to	02 15 42	03 55 28 to	03 57 23	05 28 05 to	05 29 05
01 11 47	01 12 47	02 22 16	02 23 30	04 06 22	04 07 22	05 31 03	05 32 29
01 13 56	01 16 37	02 28 48	02 31 38	04 09 47	04 10 47	05 45 15	05 46 15
01 39 29	01 40 29	02 34 55	02 38 23	04 12 26	04 14 23	05 48 57	05 49 57
01 41 55	01 43 15	02 40 32	02 41 32	04 44 59	04 46 49	05 55 30	05 57 25
01 45 23	01 46 23	02 46 12	02 47 12	04 50 07	04 51 07	06 03 55	06 04 55
01 52 03	01 53 03	02 51 10	02 57 20	04 52 43	04 57 24	06 15 49	06 17 59
01 55 02	01 57 17	03 22 00	03 29 00	05 07 51	05 16 20	06 21 20	06 22 20
02 02 10	02 03 40	03 32 19	03 33 19	05 19 00	05 20 00	06 25 55	06 26 55
02 07 39	02 08 39	03 38 24	03 39 24	05 22 10	05 23 10	06 33 52	06 34 52
			13ʰ–17ʰ Section				
13 50 49 to	13 51 56	14 36 08 to	14 37 08	15 26 54 to	15 27 54	16 54 37 to	16 57 03
13 53 37	13 54 37	14 47 49	14 48 49	15 47 31	15 48 31	16 59 47	17 00 47
13 59 14	14 00 14	14 51 02	14 52 02	15 55 10	15 57 05	17 04 23	17 05 23
14 10 17	14 11 17	14 55 12	14 58 54	16 02 00	16 21 00	17 06 41	17 07 41
14 13 24	14 15 09	15 03 06	15 04 06	16 22 50	16 23 50	17 17 04	17 18 24
14 16 31	14 17 31	15 05 10	15 06 10	16 31 22	16 32 38		
14 20 17	14 21 17	15 12 18	15 13 18	16 41 57	16 43 37		
14 22 39	14 23 39	15 21 49	15 22 49	16 45 02	16 46 02		

Table 2. Areas (1950·0) excluded due to possible east–west sidelobes

R.A. range		Dec. range		R.A. range		Dec. range	
h m	h m	° ′ ″	° ′ ″	h m	h m	° ′ ″	° ′ ″
			01ʰ–06ʰ Section				
02 34 to	02 41	−20 02 33 to	−20 09 57	04 43 to	04 50	−20 33 29 to	−20 36 00*
02 43	02 51	−20 11 13	−20 18 37	04 49	04 57	−20 33 26	−20 35 48*
02 44	02 50	−20 31 59	−20 39 24*	05 42	05 48	−19 52 11	−19 59 35
02 48	02 59	−20 36 11	−20 39 18*	05 43	05 49	−19 55 19	−20 02 43
03 13	03 19	−20 27 30	−20 34 55	05 54	06 14	−20 17 52	−20 25 16
04 08	04 18	−20 26 00	−20 33 24	06 31	06 38	−20 21 48	−20 32 16*
			13ʰ–17ʰ Section				
14 07 to	14 15	−20 02 51 to	−20 10 15	15 45 to	15 51	−19 51 31 to	−19 58 55
15 02	15 10	−20 00 19	−20 07 44	16 51	16 59	−20 03 11	−20 10 35
15 23	15 32	−19 59 49	−20 07 14	16 56	17 11	−20 23 19	−20 30 43

* Exclusion extends to the declination edge of the survey.

(c) *Sidelobes and Excluded Areas*

The sidelobes of the Molonglo cross are significant only in the north–south and east–west directions about a source. Those in the east–west direction diminish in amplitude with increasing angle from the source much more rapidly than the north–south sidelobes, which are thus the main problem. The latter have a distribution of amplitudes, but typical levels are about 2%–3%. The method adopted to eliminate north–south sidelobes and to minimize their confusing effects on other sources was to identify all sources in the vicinity of the survey that were strong enough to produce a sidelobe of over 67 mJy in the survey area, for an assumed sidelobe amplitude of (for safety) 4%. The list of possible sidelobe-producing sources was selected from a catalogue of all sources in the southern sky above about 1 Jy, which is being prepared by members of the Astrophysics Department, University of Sydney. For each source, a strip of sky 1^{m} wide in right ascension and extending over the whole declination range of the survey was excluded. Additional strips of various widths in right ascension were eliminated because of the hourly noise diode calibration signal, some interference pulses and transient equipment faults. The right ascensions excluded are listed in Table 1. The gap starting at $16^{h}02^{m}$ was due to interference as the Sun crossed the fan beams of the north–south antenna, far from the meridian.

East–west sidelobes were easily detected on the line scans. Twenty sources were strong enough to be troublesome in this way and, for each of these, a strip of sky (including the source) was eliminated. Details of the excluded areas are given in Table 2. Because the sidelobe elimination procedures result in a loss of survey sources over 1 Jy, the catalogue has been cut off at 1·0 Jy. The small pointing corrections (see Section 4) have not been applied to the boundaries of any of the excluded regions. The solid angles surveyed, allowing for all the excluded areas, are $1 \cdot 26 \times 10^{-2}$ sr for the 01^{h}–06^{h} section and $7 \cdot 51 \times 10^{-3}$ sr for the 13^{h}–17^{h} section. About 27% of the initial area has been excluded.

4. Calibration

The flux densities in the present catalogue are given on the scale due to Wyllie (1969*a*, 1969*b*). Hunstead (1972) has established a grid of subcalibrators on this scale, and 16 of these were used as calibration sources for the observing session. All were over 4 Jy, so noise and confusion errors were negligible even for a single observation. The sources were 0023−26, 0035−02, 0049−43, 0859–25, 0909–56, 0920–39, 0941–08, 1005+07, 1018−42, 1036−69, 1309−22, 1327−21, 1335−06, 1730−13, 1754−59 and 1814−63. The flux densities were given by Hunstead (1972).

The source 1730−13 gave a discrepant gain estimate, and was rejected for flux density calibration (this affected the calibration by only 1%). On some days, certain sources were not observed. The final flux density calibration was derived from 210 scans of 15 sources, and has a formal uncertainty of about $1\frac{1}{2}$%. However, this must be increased by up to 5% to allow for uncertainties in the form of the curve relating gain to declination (Hunstead 1972).

The observations of calibration sources were also used to establish the necessary pointing corrections for both position coordinates. Optical positions were available for 1335−06, 0035−02 and 0941−08 from Hunstead (1971), and 0909−56 from Hunstead *et al.* (1971). Radio positions (Hunstead 1972) were used for the remainder. The source 0049−43 gave results inconsistent with the other calibrators, and was rejected for position calibration.

The functional form adopted for the right ascension calibration correction was as described by Hunstead (1972). However, the declination correction did not follow the form given by Hunstead; a linear fit to the correction as a function of declination was found to be adequate (Robertson 1976). Since the present survey covers such a small range in declination and there is no right ascension dependence in the corrections, the derived pointing corrections and flux density calibration were constant for the whole catalogue.

5. Source Catalogue

The catalogues for the 01^h–06^h and 13^h–17^h sections are given in Tables 3 and 4 respectively. The Molonglo catalogue number (column 1) is formed from the 1950 coordinates by truncating the minutes of right ascension and the tenths of degrees of declination. When two sources have the same catalogue number they are given suffixes A and B in decreasing order of catalogued flux density. An asterisk in column 2 indicates that the source is listed in the MC1 catalogue (Davies *et al.* 1973), while the letter U following the asterisk indicates that the identification is not certain. The MC1 list ceases at $16^h 48^m$.

Columns 3–6 list the coordinates and their r.m.s. errors calculated from

$$\sigma_\alpha = \{(93\cdot 8/F)^2 + 0\cdot 21^2\}^{\frac{1}{2}} \text{ sec. time}, \qquad \sigma_\delta = \{(1540/F)^2 + 3^2\}^{\frac{1}{2}} \text{ sec. arc},$$

where F is the catalogued flux density in mJy (see Section 8). In some cases the errors are followed by a plus sign, indicating that the error should be increased (in a few cases substantially) because of extension of the source or for some other reason. In these cases, further information is given in the notes to Tables 3 and 4.

Columns 7 and 8 give the flux density in mJy, and its r.m.s. error σ calculated from the formula (see Section 6 below)

$$\sigma = \{18\cdot 20^2 + (F/25)^2\}^{\frac{1}{2}} \text{ mJy}.$$

Again a plus sign indicates that the likely error is larger than the tabulated value.

Column 9 contains references to numbered notes which may be found at the end of Table 4. It may also contain one or more of the following short comments: *Integ.*, which indicates that an integrated flux density is given (see Section 3*b*); *Fig. N*, which signifies that the source is shown on a contour map in Fig. *N*; *Missed by program*, which indicates those sources which were not found by the source fitting program, and have been fitted manually on the line scans (see Section 3*b*). Four of the sources appear in the Bologna B1 catalogue (Braccesi *et al.* 1965) and are indicated in column 9 with the prefix B1. These references have been taken from the MC1 list. Three of the sources are included in the Parkes 2700 MHz survey (Bolton *et al.* 1975; Wall *et al.* 1976) and are distinguished simply by the note PKS.

Table 3. Molonglo deep sky survey at −20°: 01^h–06^h Section

(1) Molonglo catalogue number	(2)	(3) R.A. (h m s)	(4) Position (1950·0) RMS error	(5) Dec. (° ′ ″)	(6) RMS error	(7) S_{408} (mJy)	(8) RMS error	(9) Notes
0104−204		01 04 07·1	0·9	−20 26 59	14	110	19	
0108−204	*	01 08 56·9	0·3	−20 26 57	4	633	31	
0109−204	*	01 09 35·5	0·4	−20 24 03	6	286	21	
0110−203	*	01 10 14·7	0·3	−20 20 14	4	524	28	
0113−201		01 13 05·5	0·5	−20 07 22	8	206	20	
0113−202		01 13 21·4	0·9	−20 17 00	14	111	19	
0117−202		01 17 20·0	0·4	−20 14 17	7	255	21	
0118−206	*	01 18 43·3	0·3	−20 40 53	4	580	29	
0118−202		01 18 56·4	0·4	−20 14 05	7	242	21	
0120−204	*	01 20 20·6	0·6	−20 25 11	10	162	19	

Table 3 (*Continued*)

(1) Molonglo catalogue number	(2)	(3) R.A. h m s	(4) Position (1950·0) RMS error	(5) Dec. ° ′ ″	(6) RMS error	(7) S_{408} (mJy)	(8) RMS error	(9) Notes
0120−200		01 20 39·2	0·7	−20 02 47	11	140	19	
0122−203	*	01 22 52·5	0·4	−20 19 10	7	263	21	
0123−201		01 23 19·8	0·9	−20 08 53	14	111	19	
0123−204	*	01 23 34·3	0·2	−20 26 16	4	791	37	
0124−200		01 24 53·2	0·9	−20 00 23	15	105	19	
0125−201	*	01 25 05·6	0·2	−20 11 45	3	992	44	
0125−203		01 25 45·3	0·9	−20 19 49	14	111	19	
0126−206		01 26 04·4	0·8	−20 37 07	13	123	19	
0128−205	*	01 28 59·0	0·3	−20 35 34	4	604	30	
0129−204		01 29 13·3	0·9	−20 28 49	15	104	19	
0130−203	*	01 30 01·4	0·4	−20 19 10	5	335	23	
0130−202		01 30 17·9	0·7	−20 16 49	11	142	19	
0130−200		01 30 23·8	1·1	−20 03 31	18	88	19	
0131−203		01 31 00·3	0·9	−20 18 56	15	107	19	
0131−200		01 31 36·3	0·7	−20 04 59	11	140	19	
0132−202		01 32 28·5	0·9	−20 16 41	15	104	19	
0132−204		01 32 44·5	0·6+	−20 27 50	10+	158	19+	Fig. 1, Notes 4, 5
0133−204	*	01 33 14·1	0·2	−20 24 10	4	730	34	PKS
0133−201		01 33 20·2	0·5	−20 07 21	9	187	20	
0134−206		01 34 02·6	0·7	−20 39 36	12	137	19	
0135−200	*	01 35 24·6	0·4	−20 03 05	6	309	22	
0136−203		01 36 49·1	0·8	−20 20 41	13	121	19	
0137−200	*	01 37 20·1	0·4	−20 04 38	6	285	21	
0137−203		01 37 48·8	0·8+	−20 21 35	13	121	19	Notes 5, 7, 15
0137−204		01 37 52·0	0·8	−20 25 58	14	115	19	Notes 5, 11, 15
0139−202	*	01 39 19·3	0·5	−20 16 06	9	189	20+	Note 4
0141−204		01 41 31·0	0·8	−20 29 45	13	126	19	
0143−201		01 43 27·4	0·5	−20 06 42	9	193	20	
0144−200		01 44 53·3	1·1	−20 03 12	18	88	19	
0147−201	*U	01 47 26·3	0·4	−20 06 59	6	295	22	
0148−204		01 48 01·0	0·9+	−20 28 08	14	113	19	Missed by program
0148−202	*	01 48 14·5	0·4	−20 13 59	6	268	21	
0151−199		01 51 00·5	1·0	−19 59 22	16	100	19	
0153−201		01 53 59·5	0·5+	−20 06 18	8+	224	20+	Integ., Fig. 2
0158−205		01 58 07·2	1·0	−20 33 57	17	92	19	
0159−205		01 59 18·6	0·9	−20 33 07	15	102	19	
0159−202	*	01 59 21·3	0·6	−20 16 17	10	169	19	
0159−200	*U	01 59 52·2	0·5	−20 03 01	8	213	20	
0201−206		02 01 28·1	0·3	−20 36 34	5	452	26	
0203−205		02 03 57·7	0·6	−20 31 52	10	158	19	
0209−200	*	02 09 12·4	0·5	−20 01 26	9	186	20	
0209−204		02 09 42·9	0·5	−20 28 24	8	197	20	
0210−206		02 10 06·7	0·3+	−20 39 28	5+	338	23+	Integ., Fig. 3, Note 12
0210−204		02 10 19·3	0·7	−20 26 17	11	151	19	
0211−206A		02 11 03·6	0·4+	−20 38 43	6+	317	22+	Integ., Fig. 3, Note 6
0211−206B		02 11 24·0	0·8+	−20 37 59	12+	129	19+	Fig. 3, Notes 5, 13, 15
0212−204	*	02 12 19·6	0·2	−20 29 55	4	767	36	
0214−201		02 14 00·6	0·7	−20 08 08	12	135	19	
0217−200		02 17 18·7	1·0+	−20 00 25	16	98	19	Missed by program
0218−205	*	02 18 04·3	0·5	−20 33 53	8	220	20+	Notes 2, 14
0220−205		02 20 13·3	0·6	−20 31 37	10	157	19	
0221−200		02 21 18·0	0·9	−20 02 25	15	102	19	
0224−206		02 24 22·3	1·0	−20 38 50	16	98	19	
0228−202	*	02 28 27·2	0·4	−20 14 40	6	278	21	
0231−199		02 31 46·1	1·0	−19 59 54	16	99	19	

Table 3 (*Continued*)

(1) Molonglo catalogue number	(2)	(3) Position (1950·0) R.A. h m s	(4) RMS error	(5) Dec. ° ′ ″	(6) RMS error	(7) S_{408} (mJy)	(8) RMS error	(9) Notes
0232−202	*	02 32 14·8	0·4	−20 14 32	6	305	22	
0232−204	*	02 32 57·7	0·4	−20 24 03	7	245	21	
0233−205		02 33 24·3	0·9	−20 30 17	15	102	19	
0239−202A	*	02 39 33·7	0·4	−20 17 57	6	310	22	
0239−202B	*	02 39 49·0	0·4	−20 12 15	7	258	21	
0244−204		02 44 44·7	0·8	−20 25 36	12	129	19	
0245−201		02 45 14·0	0·7	−20 07 54	11	142	19	
0247−204		02 47 29·6	0·6	−20 27 54	9	173	19	
0250−203		02 50 36·6	1·0	−20 21 42	17	94	19	
0257−205		02 57 37·4	0·5	−20 34 39	8	199	20	
0258−203		02 58 27·7	0·9	−20 23 15	15	103	19	
0259−203		02 59 34·5	0·8	−20 23 29	13	119	19	
0300−205	*	03 00 31·9	0·6	−20 34 43	9	182	20	
0300−203		03 00 59·4	0·6	−20 18 19	11	153	19	
0303−205	*	03 03 06·0	0·2	−20 35 41	4	738	35	
0308−199	*	03 08 17·6	0·4	−19 59 56	7	265	21	
0310−201		03 10 34·1	1·0	−20 09 15	16+	95	19+	Notes 3, 4
0310−204		03 10 42·9	0·8	−20 27 47	13	122	19	
0311−203		03 11 49·9	0·9	−20 18 22	14	110	19	
0315−204		03 15 27·7	0·6	−20 25 09	9	175	19	
0315−200		03 15 28·9	0·6	−20 05 09	10	163	19	
0315−201		03 15 50·6	1·1	−20 08 53	17+	90	19+	Notes 3, 5, 14
0316−203		03 16 10·2	0·5	−20 23 15	8	199	20	
0316−200	*	03 16 42·2	0·4	−20 04 43	6	327	22	
0319−203		03 19 11·3	1·0+	−20 22 07	17	93	19	Missed by program
0319−201	*	03 19 19·6	0·3	−20 09 38	5	399	24	B1 0319−20
0319−199	*	03 19 49·2	0·6	−19 58 22	10	166	19	
0320−202		03 20 38·8	1·0	−20 12 05	17	93	19	
0321−203	*	03 21 41·4	0·5	−20 20 32	8	219	20	
0321−204		03 21 49·7	1·0	−20 29 32	17	94	19	
0330−204		03 30 01·3	1·0	−20 26 23	16	98	19	
0333−201	*	03 33 25·5	0·4	−20 07 29	6+	319	22+	Integ., Note 3
0333−202	*	03 33 45·6	0·6	−20 13 33	9	181	20	
0334−200	*	03 34 39·9	0·3	−20 05 55	4	517	28	
0334−203		03 34 49·2	0·7	−20 18 52	11	148	19	
0337−202		03 37 45·7	0·5+	−20 17 11	8+	198	20+	Fig. 4, Notes 5, 13, 15
0337−203		03 37 55·6	0·6+	−20 20 21	9+	176	20+	Fig. 4, Notes 5, 13, 15
0340−201		03 40 17·4	1·0+	−20 09 33	17	93	19+	Fig. 5, Note 4
0341−200	*	03 41 50·4	0·3	−20 01 54	4+	484	27+	Integ., Note 3
0342−201	*	03 42 27·8	0·4	−20 10 24	7	263	21	
0343−200		03 43 50·1	1·0	−20 02 00	16	99	19	
0344−204	*U	03 44 13·8	0·4	−20 28 03	6	303	22	
0345−200		03 45 06·7	0·7	−20 00 25	11	139	19	
0345−199		03 45 31·4	0·6	−19 58 04	10	168	19	
0345−206	*	03 45 41·6	0·2	−20 36 44	3	994	44	
0346−205		03 46 29·8	1·0+	−20 34 04	17	94	19	Missed by program
0348−199		03 48 38·9	0·4+	−19 58 23	6+	329	22+	Integ., Fig. 6, Note 6
0349−201	*	03 49 28·5	0·4	−20 07 15	7	252	21	
0349−202		03 49 50·2	0·4	−20 12 34	7	257	21	
0351−200		03 51 59·4	1·0	−20 01 19	16	95	19	
0353−203		03 53 01·9	0·7	−20 20 03	11	149	19	
0353−204	*	03 53 05·3	0·3	−20 28 22	5	418	25	
0354−202	*	03 54 22·6	0·4	−20 14 57	6	315	22	
0354−200	*	03 54 45·7	0·4	−20 05 55	6	281	21	
0359−199	*	03 59 33·8	0·4	−19 56 19	7	238	21	

Table 3 (*Continued*)

(1) Molonglo catalogue number	(2)	(3) R.A. h m s	(4) Position (1950·0) RMS error	(5) Dec. ° ′ ″	(6) RMS error	(7) S_{408} (mJy)	(8) RMS error	(9) Notes
0400−199		04 00 46·6	1·0+	−19 56 48	16	98	19	Missed by program
0403−202		04 03 02·3	0·5	−20 13 55	8+	218	20	Notes 3, 14
0403−206		04 03 29·5	0·9	−20 36 55	15	102	19	
0407−199		04 07 28·1	0·4	−19 55 53	7	252	21	
0411−201		04 11 15·1	0·6	−20 09 14	10	154	19	
0415−200		04 15 07·0	0·9	−20 02 10	14	109	19	
0418−202	*	04 18 08·2	1·1	−20 14 23	17	90	19	
0420−203		04 20 22·9	0·5+	−20 21 58	8+	220	20+	Integ., Fig. 7, Note 13
0420−200		04 20 46·0	1·1	−20 04 06	17	90	19	
0421−203		04 21 51·4	0·6	−20 19 48	10	169	19	
0422−199	*	04 22 34·0	0·3	−19 56 43	5	455	26	
0422−202		04 22 37·6	1·0	−20 15 40	16	96	19	
0423−200	*	04 23 18·6	0·7	−20 04 53	12	132	19	
0423−199	*	04 23 32·6	0·2	−19 57 16	4	834	38	
0424−203	*	04 24 20·6	0·3	−20 22 52	4	678	33	B1 0424−20
0424−202		04 24 50·4	0·4+	−20 16 39	6+	281	21+	Integ., Fig. 8, Note 6
0427−205A		04 27 17·0	0·7	−20 32 14	11	148	19	
0427−205B		04 27 42·1	0·8	−20 35 07	14	114	19	
0427−199		04 27 54·6	0·8	−19 57 18	13	121	19	
0431−200	*	04 31 21·9	0·6	−20 05 58	9	183	20	
0431−204		04 31 23·4	0·5	−20 27 19	9	189	20	
0431−199	*	04 31 52·0	0·5	−19 58 54	8	194	20	Note 5
0431−202		04 31 53·6	0·7	−20 12 16	11	139	19	
0431−203	*	04 31 57·4	0·4	−20 21 38	7	240	21	
0433−202		04 33 44·7	0·6	−20 16 48	10	167	19	
0435−202		04 35 00·0	0·6	−20 17 44	10	155	19	
0435−205	*	04 35 01·2	0·3	−20 33 05	4	657	32	
0436−199		04 36 37·4	0·7+	−19 55 58	12+	133	19	Note 4
0436−203	*	04 36 39·7	0·2	−20 18 22	3	874	39	PKS
0436−201	*	04 36 47·8	0·5	−20 09 17	8	216	20	
0440−204		04 40 00·0	1·0+	−20 26 35	16	95	19	Missed by program
0441−204		04 41 07·2	0·5	−20 25 34	9	189	20	
0442−200		04 42 06·2	0·6	−20 04 19	10	157	19	
0442−202		04 42 17·6	0·7	−20 15 57	12	132	19	
0442−201		04 42 41·1	0·8	−20 06 50	13	118	19	
0444−204		04 44 29·0	0·5	−20 25 21	9	187	20	
0444−199		04 44 46·6	0·8	−19 56 44	13	119	19	
0449−200		04 49 02·5	0·9	−20 05 26	15	108	19	
0449−199	*	04 49 06·8	0·4	−19 59 55	7	239	21	
0452−199		04 52 33·0	1·0	−19 57 19	16	96	19	
0457−203		04 57 35·8	0·6	−20 22 57	10	169	19	
0457−205	*	04 57 53·2	0·2	−20 34 29	4	737	35	
0500−202		05 00 41·3	0·8	−20 13 37	13	126	19	
0503−200		05 03 28·4	1·1	−20 03 32	17	90	19	
0505−201		05 05 37·2	0·6	−20 11 30	10	169	19	
0506−199	*	05 06 07·0	0·3	−19 59 02	4	462	26	
0507−201		05 07 28·5	0·9	−20 11 48	14	109	19	
0507−204	*	05 07 29·8	0·5	−20 28 09	8	197	20	
0516−200		05 16 38·5	1·0	−20 00 08	16	96	19	
0516−199		05 16 59·4	1·1	−19 58 14	17	91	19	Note 5
0517−200		05 17 44·2	0·4	−20 03 38	7	266	21	
0520−203		05 20 42·5	0·7	−20 19 55	12	138	19	
0520−205	*	05 20 47·6	0·4	−20 34 06	6	293	22	
0521−204	*	05 21 28·3	0·4	−20 24 50	6	312	22	
0523−202	*	05 23 17·0	0·2+	−20 13 45	4+	840	38+	Integ., Fig. 9, Note 6

Table 3 (*Continued*)

(1) Molonglo catalogue number	(2)	(3) Position (1950·0) R.A. h m s	(4) RMS error	(5) Dec. ° ′ ″	(6) RMS error	(7) S_{408} (mJy)	(8) RMS error	(9) Notes
0523−205		05 23 20·4	0·8	−20 32 29	13	124	19	
0526−203	*	05 26 52·7	0·3	−20 23 05	4	512	27	
0527−200		05 27 02·5	0·5+	−20 03 04	9+	187	20	Note 4
0529−201		05 29 13·2	0·9	−20 07 38	14	111	19	
0530−203		05 30 07·8	0·7	−20 18 13	11	151	19	
0530−199	*	05 30 19·4	0·4	−19 59 16	6	295	22	
0530−205	*	05 30 58·9	0·4	−20 32 43	6	280	21	
0534−201	*	05 34 13·7	0·5	−20 07 19	8	207	20	
0535−201		05 35 13·3	1·0	−20 09 14	16	100	19	
0536−202		05 36 25·2	0·8	−20 13 10	12	128	19	
0536−205		05 36 32·1	0·7	−20 33 44	11	146	19	Note 5
0537−205		05 37 16·5	0·9	−20 30 38	14	113	19	
0537−201		05 37 22·2	1·1	−20 08 53	17	90	19	
0540−199		05 40 56·9	0·9+	−19 57 07	15	108	19	Missed by program
0541−202		05 41 41·0	0·7	−20 15 54	12	137	19	
0542−205		05 42 36·2	0·7	−20 30 33	12	134	19	
0544−202		05 44 17·6	0·8	−20 13 02	14	115	19	
0546−202	*	05 46 17·0	0·4	−20 12 13	6	323	22	
0546−205	*	05 46 20·7	0·3	−20 33 06	5	411	25	
0547−203		05 47 44·7	1·0	−20 19 27	16	100	19	
0548−203		05 48 30·1	1·1	−20 19 38	17	90	19	
0550−204		05 50 47·4	0·5	−20 28 09	8	206	20	
0553−205		05 53 10·1	0·3	−20 30 17	5	340	23	
0553−203		05 53 15·5	0·9	−20 21 58	15	107	19	
0558−200		05 58 57·6	0·8	−20 04 38	12	128	19	
0559−202		05 59 02·0	1·0+	−20 15 17	16	95	19	Missed by program
0559−200		05 59 44·9	0·9	−20 05 16	14	109	19	
0602−202		06 02 47·0	0·6+	−20 15 45	9	177	20+	Notes 2, 4
0603−204		06 03 27·4	0·5	−20 29 26	9	190	20	
0605−202		06 05 17·3	0·5	−20 13 10	8	200	20	
0606−201		06 06 04·9	0·5	−20 06 40	9	193	20	
0606−198	*	06 06 28·8	0·3	−19 52 11	4	601	30	B1 0606−20
0607−205	*	06 07 21·8	0·3	−20 32 33	4	672	32	
0609−202		06 09 25·2	0·7	−20 16 08	11	147	19	
0611−201		06 11 18·1	0·7	−20 11 34	12	137	19	
0612−200		06 12 12·1	0·6	−20 04 35	9	173	19	
0615−201	*	06 15 02·4	0·4+	−20 06 10	6+	321	22+	Integ., Note 6
0618−199		06 18 22·2	1·0+	−19 54 20	17	93	19	Missed by program
0618−200		06 18 58·8	0·9+	−20 01 40	14+	110	19+	Notes 5, 14, 15
0619−200		06 19 17·3	0·9+	−20 01 38	15+	104	19+	Notes 4, 15
0621−203		06 21 10·1	0·8	−20 22 56	13	120	19	Note 5
0624−203	*	06 24 09·4	0·3+	−20 19 52	5+	424	25+	Integ., Note 3
0625−201		06 25 51·8	0·5	−20 10 23	8	206	20	
0627−199	*	06 27 14·0	0·3	−19 57 16	4	516	28	B1 0627−19, PKS
0627−202		06 27 14·6	1·0	−20 12 17	16	95	19	
0627−201	*	06 27 51·6	0·3+	−20 07 47	4+	477	26+	Integ., Fig. 10, Note 6
0628−200	*	06 28 33·3	0·3	−20 03 04	5	401	24	
0628−202		06 28 38·8	1·1+	−20 15 50	17	90	19	Missed by program
0628−201	*	06 28 55·9	0·3	−20 07 50	5	345	23	
0629−202		06 29 49·2	0·7	−20 16 28	12	134	19	
0629−205	*	06 29 51·8	0·3	−20 31 02	5	353	23+	Note 5
0630−203		06 30 34·9	1·0+	−20 22 49	16	96	19	Missed by program
0631−199		06 31 32·7	0·7	−19 57 33	11	140	19	
0632−201		06 32 01·0	0·8	−20 06 47	13	119	19	
0635−203		06 35 12·3	1·0	−20 18 08	16	101	19	
0636−198		06 36 05·3	0·9	−19 51 08	14	110	19	
0638−199	*	06 38 26·0	0·3	−19 57 20	4	472	26	

Table 4. Molonglo deep sky survey at −20°: 13h–17h Section

(1) Molonglo catalogue number	(2)	(3) Position (1950·0) R.A. h m s	(4) RMS error	(5) Dec. ° ′ ″	(6) RMS error	(7) S_{408} (mJy)	(8) RMS error	(9) Notes
1345−202	*	13 45 42·5	0·4	−20 14 56	6	295	22	
1345−203		13 45 43·7	0·8	−20 20 42	13	118	19	
1347−197		13 47 36·8	0·6	−19 45 29	10	155	19	
1349−201		13 49 40·4	1·0+	−20 08 58	16	96	19	Missed by program
1352−197	*	13 52 01·1	0·2	−19 46 50	4	762	36	
1352−204A	*	13 52 39·9	0·5	−20 26 09	8	219	20	
1352−204B		13 52 59·0	0·6	−20 24 05	11	153	19	
1352−199	*	13 52 59·7	1·1	−19 56 57	18	88	19	
1356−199	*	13 56 12·8	0·3	−19 57 54	5	434	25	
1356−201		13 56 54·2	0·7	−20 09 28	12	131	19	
1401−202		14 01 04·4	1·0+	−20 12 08	17	93	19	Missed by program
1402−198		14 02 12·0	1·1	−19 50 43	17	91	19	
1402−202		14 02 26·7	0·7	−20 14 28	12	135	19	
1403−203		14 03 46·0	0·8	−20 23 39	13	125	19	
1404−199		14 04 10·4	0·4+	−19 58 51	6+	290	22+	Integ., Note 1
1405−198		14 05 21·4	0·7	−19 49 55	11	151	19	
1407−202		14 07 53·2	0·5	−20 16 58	8	210	20	
1408−202		14 08 27·2	0·8	−20 17 48	13	118	19	
1411−202		14 11 40·3	0·4	−20 13 32	6	273	21	
1411−198		14 11 50·2	0·6	−19 49 05	10	165	19	
1417−199		14 17 35·4	0·6	−19 58 48	9	182	20	
1418−198B		14 18 14·8	1·1	−19 48 33	17	91	19	
1418−198A		14 18 54·7	0·3	−19 48 01	5	348	23	
1419−200		14 19 25·6	0·6	−20 05 33	9	178	20	
1419−201		14 19 27·8	0·4	−20 11 00	6	268	21	
1421−198		14 21 48·3	1·0	−19 51 37	16	100	19	
1421−200		14 21 55·5	0·7	−20 05 51	12	131	19	Fig. 11
1422−200		14 22 24·8	0·9+	−20 04 41	14+	113	19+	Fig. 11, Notes 4, 5
1424−199		14 24 02·5	0·8	−19 56 08	12	129	19	
1424−198		14 24 43·0	0·7	−19 48 36	11	139	19	
1425−198		14 25 09·5	0·4	−19 52 20	6	268	21	
1425−204		14 25 28·0	0·4	−20 26 35	6	297	22	
1425−197	*	14 25 49·3	0·5	−19 45 25	8	215	20	
1426−202		14 26 31·1	0·9	−20 16 15	15	106	19	
1427−199	*	14 27 28·2	0·4	−19 58 05	6	331	23	
1429−201		14 29 16·4	0·9+	−20 10 28	14	110	19	Missed by program
1430−204		14 30 03·3	0·9	−20 25 33	14	112	19	
1431−202	*	14 31 23·9	0·3	−20 14 52	4	514	27	
1433−201	*	14 33 48·4	0·2+	−20 10 28	4+	756	35+	Integ., Fig. 12, Note 6
1434−201		14 34 35·4	0·5	−20 09 42	8	207	20	
1434−203	*	14 34 37·0	0·3	−20 22 10	5	442	25	
1437−203B		14 37 21·5	0·8+	−20 21 20	12	130	19	Notes 5, 15
1437−203A		14 37 42·5	0·5+	−20 19 42	8	218	20	Notes 5, 15
1438−198	*	14 38 32·0	0·4	−19 52 02	6	275	21	
1441−200	*	14 41 57·0	0·3	−20 01 47	5	375	24	
1443−198	*	14 43 58·6	0·2	−19 51 04	3	980	43	
1444−200	*	14 44 10·9	0·4	−20 05 23	6	312	22	
1444−199	*	14 44 23·4	0·3	−19 56 43	4	470	26	
1444−203		14 44 26·9	0·5	−20 20 15	8	214	20	
1445−197	*	14 45 00·3	0·5	−19 46 16	7	227	20	
1446−202		14 46 15·4	1·1+	−20 17 48	17	91	19	Missed by program
1446−198		14 46 55·9	0·7	−19 51 01	11	149	19	
1450−204		14 50 43·1	0·9	−20 25 13	15	107	19	
1450−200		14 50 48·4	0·6	−20 00 13	10	165	19	
1455−198		14 55 01·0	0·6	−19 48 24	10	159	19	

Table 4 (*Continued*)

(1) Molonglo catalogue number	(2)	(3) R.A. h m s	(4) Position (1950·0) RMS error	(5) Dec. ° ′ ″	(6) RMS error	(7) S_{408} (mJy)	(8) RMS error	(9) Notes
1459−197	*	14 59 34·1	0·3	−19 46 04	5	443	25	
1459−202		14 59 43·4	0·5+	−20 13 19	8+	195	20+	Integ., Note 7
1500−202	*	15 00 15·8	0·3	−20 12 17	5	369	23	
1501−198		15 01 09·3	0·5	−19 49 19	7	231	20	
1507−203	*	15 07 36·9	0·3	−20 21 47	4	610	30	
1508−199	*	15 08 02·8	0·5	−19 59 33	8	203	20	
1509−198		15 09 52·9	0·8	−19 52 56	13	124	19	
1510−203	*	15 10 48·6	0·4	−20 21 49	6	302	22	
1511−204		15 11 03·2	0·6	−20 26 33	10	164	19	
1515−201		15 15 48·1	0·6	−20 11 11	10	167	19	
1516−202		15 16 39·2	0·9	−20 13 06	15	103	19	
1523−202		15 23 05·6	0·8	−20 16 50	13	123	19	
1523−203B		15 23 08·8	0·7	−20 23 12	12	133	19	
1523−203A		15 23 30·0	0·6	−20 18 52	10	162	19	
1524−201	*	15 24 08·3	0·3	−20 08 11	4	685	33	
1527−198		15 27 57·1	0·7	−19 50 06	11	148	19	
1528−199		15 28 13·3	0·9	−19 54 31	15	106	19	
1528−203	*	15 28 16·1	0·3	−20 22 50	5	436	25	
1530−199		15 30 08·7	1·0	−19 54 10	16	98	19	
1530−204		15 30 11·7	1·0	−20 25 48	16	98	19	
1532−200	*	15 32 12·8	0·2	−20 00 11	4	727	34	
1532−203		15 32 26·7	0·9	−20 22 47	15	105	19	
1535−202	*U	15 35 50·4	0·7	−20 14 03	11	143	19	
1536−200		15 36 02·2	0·7	−20 00 45	11	140	19	
1537−200	*	15 37 10·0	0·3+	−20 03 47	5+	361	23+	Fig. 13, Notes 4, 5
1538−202		15 38 42·1	0·6	−20 12 57	10	158	19	
1542−204		15 42 56·1	0·3	−20 27 05	5	403	24	
1543−198		15 43 36·1	0·5	−19 53 26	7	229	20	
1544−202		15 44 16·6	0·7	−20 12 59	12	132	19	
1544−201		15 44 29·4	0·9	−20 06 47	14	110	19	
1545−202		15 45 03·9	0·5	−20 15 22	8	204	20	
1547−204		15 47 07·1	0·7	−20 24 20	11	144	19	
1553−200B		15 53 02·1	0·6+	−20 00 37	9+	174	19+	Note 9
1553−200A	*U	15 53 54·5	0·5	−20 01 03	7	234	20+	Note 5
1554−201	*	15 54 01·2	0·4	−20 07 42	7	248	21	
1554−203		15 54 25·6	0·3+	−20 20 41	5+	434	25+	Integ., Fig. 14
1557−199		15 57 15·6	0·6	−19 59 34	10	158	19	
1558−198		15 58 16·0	0·9	−19 52 30	14	111	19	
1559−202		15 59 11·7	0·4	−20 17 49	6	296	22	
1559−203		15 59 32·8	1·0	−20 22 54	16	98	19	
1600−201		16 00 48·6	1·1	−20 07 37	17	91	19	
1600−199		16 00 49·8	0·5	−19 54 54	7	227	20	
1601−203		16 01 20·1	0·8	−20 19 48	14	116	19	
1601−201	*	16 01 46·3	0·4	−20 08 37	6	327	22	
1621−198		16 21 50·3	0·4	−19 50 31	7	245	21	
1625−198		16 25 08·1	0·7	−19 53 31	11	141	19	
1626−203		16 26 06·4	0·5	−20 20 24	8	217	20	
1626−198		16 26 09·5	0·6	−19 49 34	9	172	19	
1628−202		16 28 10·1	0·4	−20 15 54	6	285	21	
1635−203	*	16 35 08·6	0·3	−20 18 06	5	390	24	
1635−202		16 35 24·4	0·7	−20 12 29	12	135	19	
1636−201		16 36 07·4	0·9	−20 07 14	14	112	19	Fig. 15
1636−200	*	16 36 32·0	0·5+	−20 02 15	7+	229	20+	Integ., Fig. 15, Note 6
1638−202		16 38 25·6	0·4	−20 16 19	7	262	21	
1638−204		16 38 37·9	0·2	−20 24 21	4	757	35	

Table 4 (*Continued*)

(1) Molonglo catalogue number	(2)	(3) R.A. h m s	(4) Position (1950·0) RMS error	(5) Dec. ° ′ ″	(6) RMS error	(7) S_{408} (mJy)	(8) RMS error	(9) Notes
1639 − 200	*	16 39 04·6	0·2+	−20 00 00	3+	896	40+	Integ., Fig. 16, Note 8
1639 − 202		16 39 04·6	0·9	−20 16 40	14	110	19	
1641 − 204		16 41 34·8	0·8	−20 29 53	13	119	19	
1643 − 200		16 43 40·8	0·4	−20 03 05	7	248	21	
1646 − 201		16 46 42·5	0·8+	−20 06 26	13+	124	19+	Note 10
1647 − 200	*	16 47 13·6	0·3+	−20 05 00	5+	427	25+	Note 10
1647 − 202	*	16 47 36·4	0·3	−20 12 46	5	363	23	
1648 − 198B		16 48 18·4	0·4+	−19 51 32	6+	300	22+	Integ., Fig. 17
1648 − 198A		16 48 51·4	0·3	−19 51 58	4	689	33	
1649 − 200		16 49 11·5	0·2	−20 02 40	4	744	35	
1651 − 205		16 51 30·7	0·5	−20 30 14	8	201	20	
1652 − 202		16 52 08·0	0·7	−20 12 41	11	144	19	
1652 − 204		16 52 43·7	1·0+	−20 27 14	16	100	19	Missed by program
1652 − 199		16 52 50·2	0·8	−19 56 01	13	124	19	
1652 − 198		16 52 52·0	0·2	−19 50 01	4	730	34	
1654 − 200		16 54 36·1	0·4	−20 00 07	6	303	22	
1657 − 203		16 57 23·5	0·2	−20 20 39	3	865	39	
1658 − 200		16 58 37·9	0·3	−20 03 40	4	533	28	
1701 − 200		17 01 27·7	0·7	−20 00 21	11	146	19	
1701 − 203		17 01 33·1	0·5	−20 19 07	8	204	20	
1703 − 201		17 03 07·2	0·7	−20 07 48	11	143	19	
1703 − 203		17 03 28·8	0·4	−20 19 50	6	322	22	
1705 − 198		17 05 49·4	0·9+	−19 50 19	15	108	19	Missed by program
1707 − 199		17 07 59·6	0·8	−19 59 02	12	128	19	
1711 − 200		17 11 40·3	0·7	−20 03 40	12	133	19	Fig. 18
1712 − 201		17 12 03·4	1·0	−20 07 23	17	92	19	
1712 − 200		17 12 23·9	0·4+	−20 01 23	7+	248	21+	Integ., Fig. 18, Note 6
1712 − 198		17 12 53·9	0·4+	−19 53 28	7+	244	21+	Note 4
1713 − 204		17 13 47·3	0·7	−20 26 12	11	152	19	
1713 − 199		17 13 50·3	0·5	−19 56 27	8	198	20	
1719 − 205		17 19 10·5	0·5	−20 30 47	8	214	20	

Notes to Tables 3 and 4

1, Extended in both right ascension and declination
2, Extension primarily in right ascension
3, Extension primarily in declination
4, Probably extended, but integrated flux density not used (see Section 3*b*(ii))
5, Flux density obtained manually from the line scans (see Section 3*b*(iv))
6, Position given is an *approximate* centroid for two close peaks which are not resolved, by the criterion of Section 3*b*(i)
7, Position obtained manually from the line scans
8, Integrated flux density includes a small unresolved source
9, Uncertainties in position and flux density increased due to variation in background level
10, Sources 1646 − 201 and 1647 − 200 appear to be connected by a low level bridge, or to have a third source between them
11, Declination obtained manually from the line scans
12, Integrated flux density includes a small unresolved source. The position given is that of the stronger component
13, Position obtained manually from contour map
14, Possibly extended, but integrated flux density not used. (Extension less significant than for Note 4)
15, Very close to another catalogued source, but still resolved (see Section 3*b*(i))

Table 5. Details of contour maps

Fig. No.	Sources contained	Contour interval (mJy)	Comments
1	0132 − 204	15	zero level contour omitted
2	0153 − 201	20	zero level contour omitted
3	0210 − 206 0211 − 206A 0211 − 206B	30	
4	0337 − 202 0337 − 203	30	zero level contour omitted
5	0340 − 201	20	first plotted contour at 40 mJy
6	0348 − 199	20	zero level contour omitted
7	0420 − 203	15	zero level contour omitted
8	0424 − 202	20	hatched area due to stronger source 0424 − 203
9	0523 − 202	40	first plotted contour at 20 mJy; alternate contours omitted above fourth plotted
10	0627 − 201	30	zero level contour omitted; alternate contours omitted above fourth plotted
11	1421 − 200 1422 − 200	20	third source present from an excluded area (but not a sidelobe); zero level contour omitted
12	1433 − 201	60	
13	1537 − 200	30	
14	1554 − 203	30	
15	1636 − 200 1636 − 201	15	zero level contour omitted
16	1639 − 200	60	
17	1648 − 198B	25	zero level contour omitted
18	1711 − 200 1712 − 200	30	zero level contour omitted

Contour maps for some of the sources are given in Figs 1–18, and details of the maps are listed in Table 5. The sources selected for mapping were those showing extension on the line scans, or regions where several peaks occurred close together. (The distinction between these two cases is only a matter of degree, and no implications are made as to whether components of a source are physically associated or not.) Maps were obtained for the majority of suitable sources. Contour intervals are given (in Table 5) in units of peak flux density. In some cases a small contour interval has been used to show clearly the extension of the sources—this may result in several of the lowest contours being dominated by noise. The effective half-power beamshape is shown by the ellipse in the insert to each map. Integrated flux densities cannot be reliably obtained from the contour maps because of uncertainties in the background levels assessed by the contouring program.

Fig. 1 0132−204

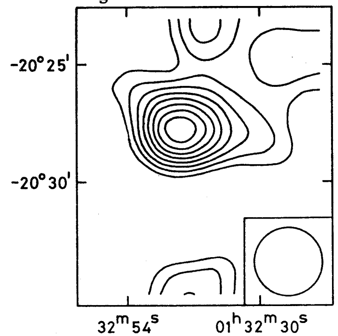

Fig. 2 0153−201

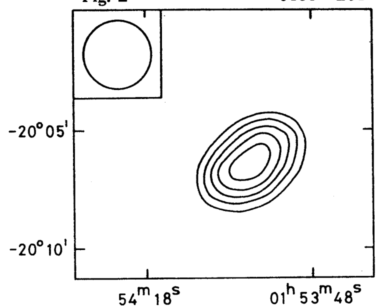

Figs 1–18 (pp. 223–6). Contour maps of the indicated Molonglo sources. (See Table 5 for details of the maps.)

Fig. 3 0210−206, 0211−206A, 0211−206B

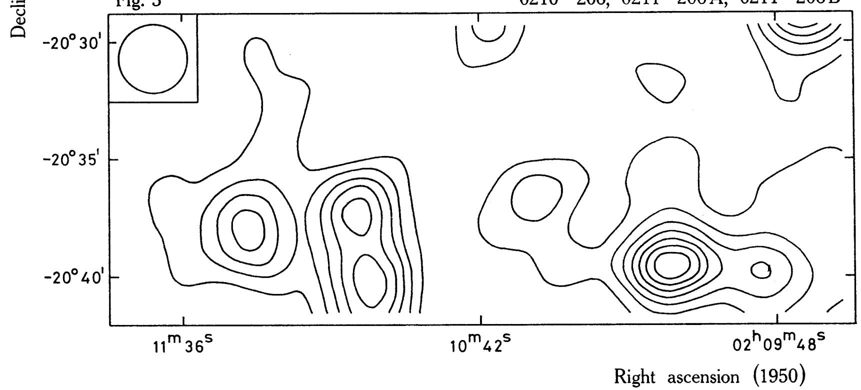

Fig. 4 0337−202, 0337−203

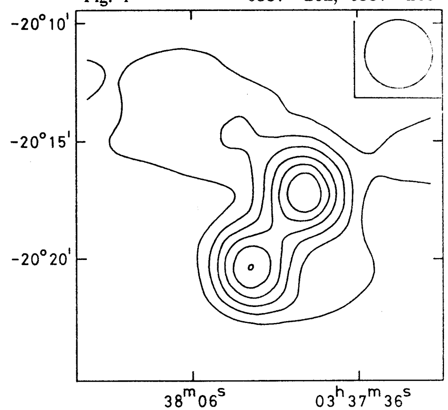

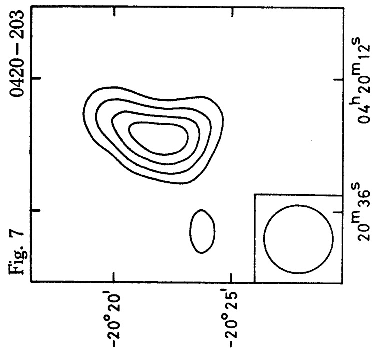

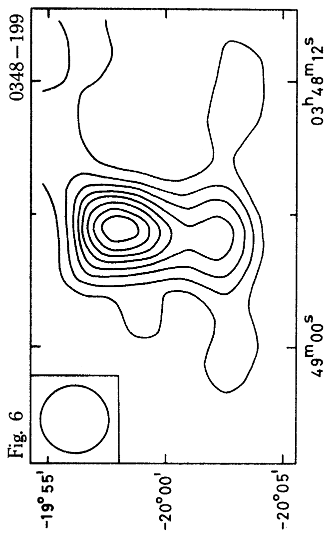

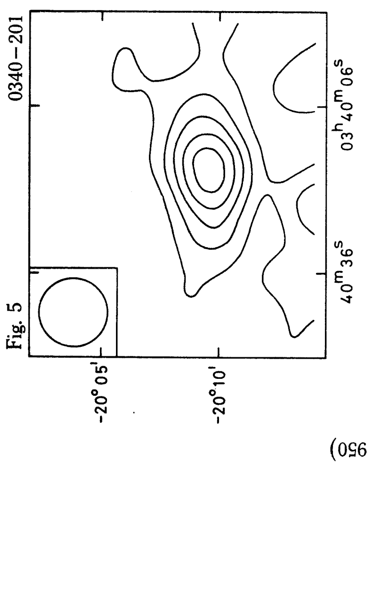

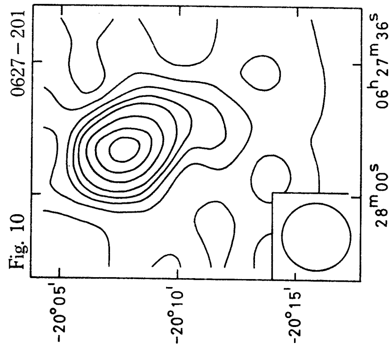

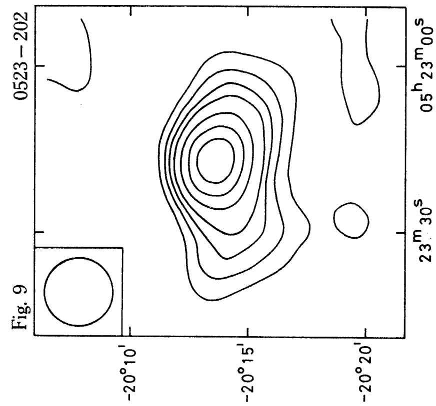

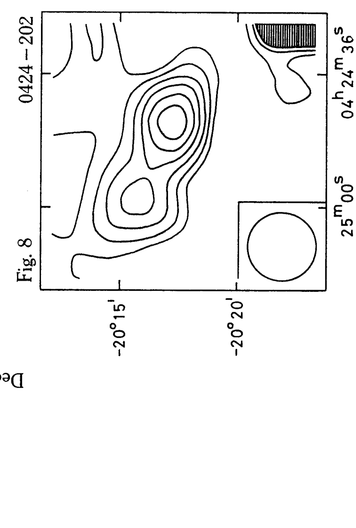

Right ascension (1950)

Declination (1950)

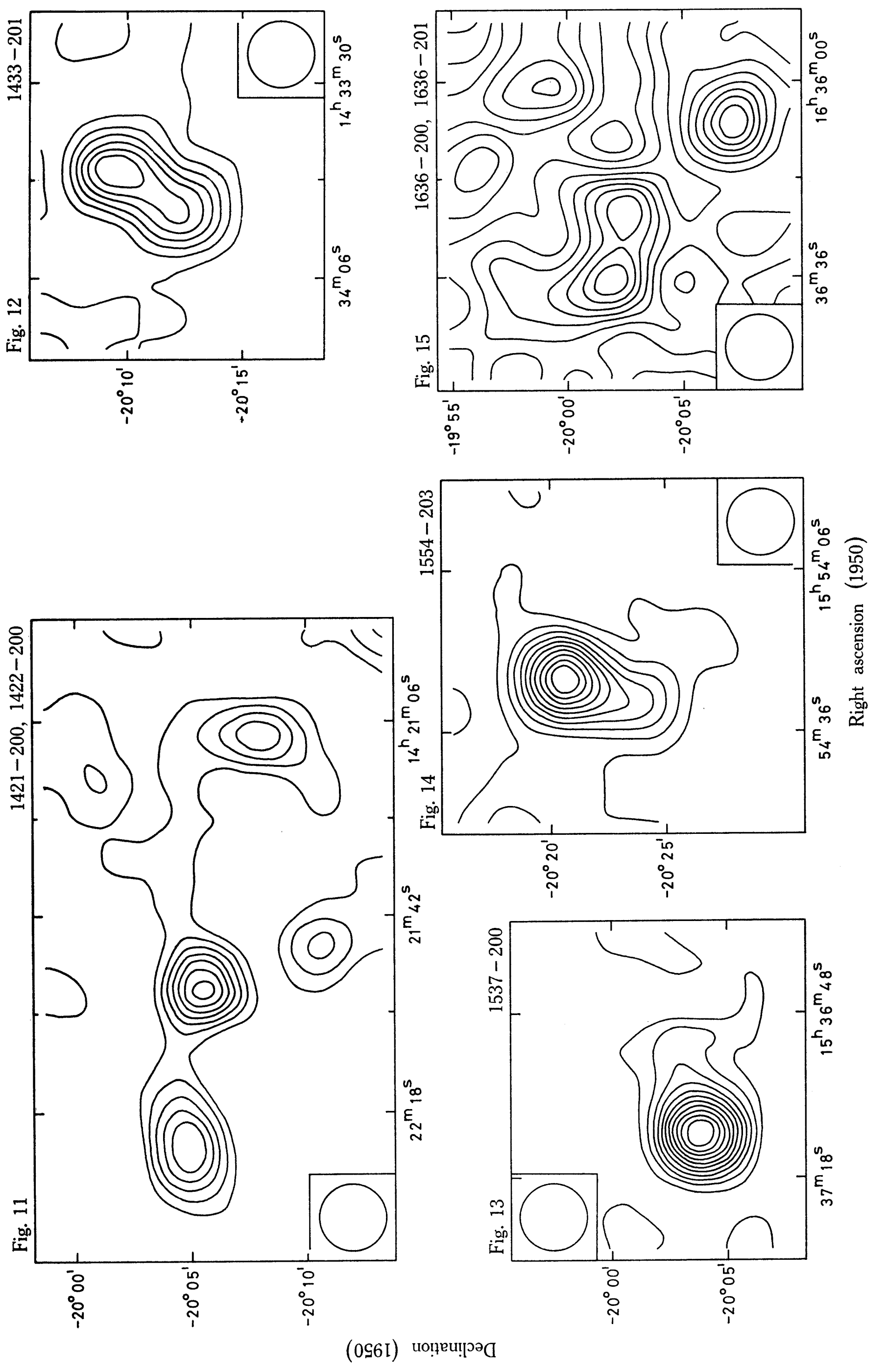
Fig. 11
1421−200, 1422−200
Fig. 12
1433−201
Fig. 13
1537−200
Fig. 14
1554−203
Fig. 15
1636−200, 1636−201
Right ascension (1950)
Declination (1950)

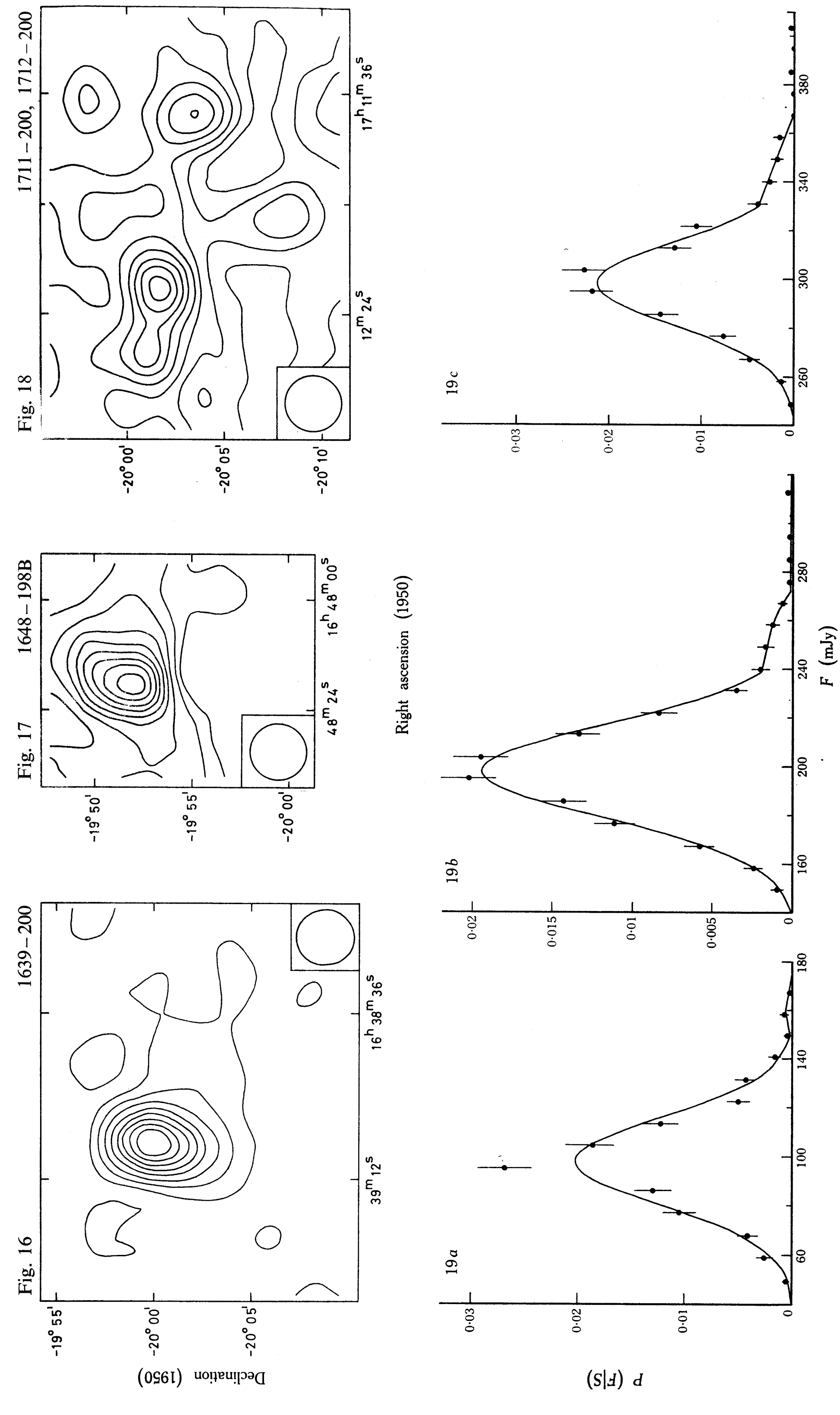
Fig. 16
1639 − 200
Fig. 17
1648 − 198B
Fig. 18
1711 − 200, 1712 − 200
Declination (1950)
Right ascension (1950)
19a
19b
19c
P (F|S)
F (mJy)

6. Error Analysis for Flux Densities

The importance of a careful error analysis for flux densities is now well established (e.g. Murdoch *et al.* 1973; Jauncey 1975). In particular, the compilation of reliable number–flux density counts requires a knowledge of the error distribution.

The principal method used to find the distribution of errors in flux density was the insertion of synthetic (Monte Carlo) sources into the averaged data records, with subsequent source fitting by the same computer program as was used to analyse the actual survey records. It was important that the Monte Carlo sources be treated in a manner as similar as possible to the catalogue sources; e.g. criterion (i) of Section 3*b* was used to decide if a Monte Carlo source was obscured. Since the Monte Carlo sources were inserted with a known amplitude, one can obtain the distribution of errors from the fitted flux densities. This includes the effects of noise, confusion and any mean bias introduced by the source fitting program, but cannot show any calibration error. The method of using the Monte Carlo sources followed the recommendation of Murdoch *et al.* (1973), in which a large number of sources are inserted at each of several chosen flux densities. For the present survey, 486 sources were inserted at 100 mJy, 726 at 200 mJy and 419 at 300 mJy.

Following the terminology of Murdoch *et al.* (1973), let S represent the true flux density of a source and F its observed flux density. The errors are described by the function $P(F \mid S)$, the probability that a source of true flux density S will be observed as F. Where confusion is significant, we require also that the specified source is the strongest one contributing to the observed flux density. If it is not, the source is classed as obscured, and does not contribute to $P(F \mid S)$. For this reason, the integral of $P(F \mid S)$ over all values of F is less than unity. The histograms of Monte Carlo results, when appropriately normalized, represent (within statistical fluctuations) the $P(F \mid S)$ distributions for three fixed values of S. The results are shown in Fig. 19 (further details are given by Robertson 1976). The error distributions show in each case a peak (due to noise and small confusion errors) and a small tail due to occasional larger confusion errors. A least squares procedure was used to fit a gaussian function to each peak region, with the fitting process truncated where the tail became appreciable in order to avoid introducing any bias. Ideally the peak of each distribution would be located at an observed flux density equal to the true flux density; any displacement of the peak from this location represents a flux density bias. The values of bias found ranged from 1 to 3 mJy with an uncertainty of 1 mJy. They are too small to require alteration of the catalogued flux densities, but they do have a marginally significant effect on the count corrections. Because the values were small, it was adequate to use a single average bias, independent of true flux density, when analysing the distributions. This bias corresponded to an underestimation of $2 \cdot 1$ mJy.

Independent standard deviations were fitted (with the constraint of the common bias), because the standard deviation can be expected to vary somewhat with true

Fig. 19 (*opposite*). Distributions of noise and confusion errors as obtained by analysis of Monte Carlo sources for true flux densities of (*a*) 100, (*b*) 200 and (*c*) 300 mJy. The standard deviations for the gaussian parts of the distributions are (*a*) $17 \cdot 6 \pm 0 \cdot 6$, (*b*) $18 \cdot 8 \pm 0 \cdot 7$ and (*c*) $17 \cdot 0 \pm 0 \cdot 8$ mJy. In the tail regions, a smooth fit to the observed points has been made. In (*b*) and (*c*) a few sources were observed with flux densities higher than shown, and are included in a low-level tail of constant height extending to $F = 360$ and 580 mJy respectively.

flux density through its confusion component. The average standard deviation was 18 mJy. Fig. 19*a* shows that the confusion tail is not significant at $S = 100$ mJy, and thus the standard deviation of the fitted gaussian curve can be used to examine the signal to noise ratio of the catalogued sources, which was 5·0 at the lower limit of 88 mJy.

Information about the relative contributions of noise and confusion was obtained by analysing a further 356 Monte Carlo sources added to records that were formed by *subtraction* of the independent scans, thus removing the effects of confusion. The r.m.s. error due to noise alone was $14\cdot6 \pm 0\cdot6$ mJy, and that due to confusion alone was $10\cdot9 \pm 1\cdot3$ mJy (for sources in the vicinity of 100–200 mJy). The latter value refers only to the gaussian part of the error distribution, and shows that confusion effects broaden this as well as producing the tail. These results show that the confusion limit of the telescope is approached but not reached by the present survey. The number of beam solid angles per source is 74, where integration of the normalized power pattern over the main beam only has been used to calculate the beam solid angle.

It is also interesting to compare the confusion contributed by the main beam with that from the sidelobes, which are expected to make an increasing contribution at lower flux densities due to the flattening of the source count curve. A calculation based on the observed percentage amplitudes of sidelobes in the excluded areas of the survey showed that sidelobes contribute about half of the total confusion near the lower limit of the catalogue.

Noise errors can also be evaluated by comparing the flux densities obtained by two independent observations of each source, as was done for the MC1–MC4 catalogues. This method does not include the effects of confusion, but does partially include random calibration errors. It was used here to provide a check on the Monte Carlo analysis and an estimate of the calibration errors. The result for the r.m.s. error due to noise alone, scaled to apply to fully averaged data, was $11\cdot9 \pm 1\cdot7$ mJy, in reasonable agreement with the value of $14\cdot6 \pm 0\cdot6$ mJy obtained from the Monte Carlo analysis. The estimate of random calibration error obtained was an r.m.s. value of $4\cdot0\% \pm 1\cdot2\%$, which applies only to gain variations on a time scale of a few days or less. It is similar to the values obtained in the previous surveys made with this instrument.

The expected reduction in the noise level relative to the MC1 survey has been achieved, provided one allows for the significant confusion error in the deep survey, which is not reduced by averaging records, and for a noise correlation between the three beams in right ascension, which reduces the improvement in signal to noise ratio from $\sqrt{3}$ to close to $\sqrt{2}$ (see Robertson 1976).

7. Completeness and Reliability of Catalogue

The definition of completeness given by Dixon and Kraus (1968) has been used by a number of authors, but it is unsatisfactory for calculating completeness above the lower limit of a survey because some sources not in the catalogue (but which should be, based on their true flux densities) are still counted towards the completeness. Sources lost because of finite angular resolution (i.e. obscured) are also counted towards the completeness.

The definition adopted here is that the completeness above a flux density limit l is equal to the number of sources having both $F \geqslant l$ and $S \geqslant l$ divided by the number of sources with $S \geqslant l$. That is, the number of sources that both are in the catalogue above the limit and should be so, based on their true flux densities, divided by the number that should be above this limit. This definition gives lower but more meaningful values of completeness. Since the true flux densities of catalogued sources are unknown, the completeness must be estimated using the error distributions to relate F and S. The calculation is given by Robertson (1976).

For the flux density limit of 88 mJy, the completeness is 87·6% ±0·7%, allowing for noise, confusion and obscuration; and 92·2% ±0·2% allowing for noise and confusion only. For a flux density limit of 125 mJy, the values are 91·2% ±0·5% and 94·1% ±0·2% respectively. These values do not allow for the possible loss of a few considerably broadened weak sources. For comparison, the completeness of a catalogue subject to pure gaussian noise, with no obscuration, and from a source population obeying a Euclidean source count law was calculated. It is 92% for a lower limit at 5 times the r.m.s. noise and 95·5% at 10 times the r.m.s. noise.

A second important property of a catalogue is its reliability, i.e. the fraction of sources included that are real. A definition of reliability is given by Dixon and Kraus (1968) but it is not sufficiently restrictive for, in the case of their (approximate) total reliability, sources with observed flux densities many times larger than their true flux density can still be counted towards the reliability. The definition used in the present paper is that a source is real if its observed flux density F is no greater than twice its true flux density S. This is arbitrary but reasonable. The reliability of a catalogue above a limit l is then defined as the number of sources having both $F \geqslant l$ and $S \geqslant \frac{1}{2}F$ divided by the number of sources with $F \geqslant l$. It is not possible to calculate precise values for the reliability. However, the discussion by Robertson (1976) shows that the catalogue is highly reliable, especially above about 100 mJy.

A commonly used rule of thumb is that the lower limit of a survey should be at least five times the r.m.s. error. It should be noted, however, that the important quantities such as completeness and reliability also depend on the underlying source count curve, even for noise-limited observations. Since surveys are now reaching values of flux density where the source count slope is significantly flatter than before, it may be desirable to set the lower limit by using quantities such as completeness and reliability. This has the additional advantage that the quality of confusion-limited surveys can be directly compared with that of noise-limited surveys, in spite of the skew nature of the confusion error distribution which renders r.m.s. errors less meaningful.

8. Estimation of Errors in Source Positions

The formula for position uncertainty in either coordinate was assumed to be of the form

$$\sigma^2 = A^2/F^2 + B^2,$$

where the first term includes the effects of noise and confusion, and the second term is due to random calibration errors. Studies using the Monte Carlo and reobservation methods showed that the noise and confusion term alone gives $\sigma_\alpha = 13''\cdot 2 \pm 1''$ and $\sigma_\delta = 15''\cdot 4 \pm 1''$ at 100 mJy, while the r.m.s. calibration errors can be taken as 3″ in both coordinates. The uncertainty due to confusion is comparable with that from noise, as for the flux density errors. In using these r.m.s. errors, it must be borne in mind that the distribution is not strictly gaussian, and there is a somewhat enhanced probability of occasional large errors due to large ionospheric effects or confusion.

Acknowledgments

I am grateful to Professor B. Y. Mills for advice during all stages of this work and to Dr D. F. Crawford, Dr H. S. Murdoch, Dr J. N. Clarke and Dr D. L. Jauncey for helpful discussions. The work was supported by the Australian Research Grants Committee, the Sydney University Research Grants Committee and the Science Foundation for Physics within the University of Sydney. I acknowledge the receipt of a Commonwealth Postgraduate Studentship (1971–74) and a Tutorship within the University of Sydney (1975–76).

References

Bolton, J. G., Shimmins, A. J., and Wall, J. V. (1975). *Aust. J. Phys. Astrophys. Suppl.* No. 34.
Braccesi, A., *et al.* (1965). *Nuovo Cimento* B **40**, 267.
Clarke, J. N., Little, A. G., and Mills, B. Y. (1976). *Aust. J. Phys. Astrophys. Suppl.* No. 40.
Davies, I. M., Little, A. G., and Mills, B. Y. (1973). *Aust. J. Phys. Astrophys. Suppl.* No. 28.
Dixon, R. S., and Kraus, J. D. (1968). *Astron. J.* **73**, 381.
Hunstead, R. W. (1971). *Mon. Not. R. Astron. Soc.* **152**, 277.
Hunstead, R. W. (1972). *Mon. Not. R. Astron. Soc.* **157**, 367.
Hunstead, R. W., Lasker, B. M., Mintz, Betty, and Smith, M. G. (1971). *Aust. J. Phys.* **24**, 601.
Jauncey, D. L. (1975). *Annu. Rev. Astron. Astrophys.* **13**, 23.
Munro, R. E. B. (1971). *Aust. J. Phys.* **24**, 263.
Murdoch, H. S., Crawford, D. F., and Jauncey, D. L. (1973). *Astrophys. J.* **183**, 1.
Robertson, J. G. (1976). Ph.D. Thesis, University of Sydney.
Robertson, J. G. (1977*a*). *Aust. J. Phys.* **30**, 231.
Robertson, J. G. (1977*b*). *Aust. J. Phys.* **30**, 241.
Sutton, J. M., Davies, I. M., Little, A. G., and Murdoch, H. S. (1974). *Aust. J. Phys. Astrophys. Suppl.* No. 33.
Wall, J. V., Wright, A. E., and Bolton, J. G. (1976). *Aust. J. Phys. Astrophys. Suppl.* No. 39.
Wyllie, D. V. (1969*a*). *Mon. Not. R. Astron. Soc.* **142**, 229.
Wyllie, D. V. (1969*b*). *Proc. Astron. Soc. Aust.* **1**, 234.

Manuscript received 12 April 1976, revised 12 August 1976